

Table II. Extended Hückel Parameters

orbital	H_{ii} , eV	ζ_1^a	ζ_2	c_1^a	c_2
Si 3s	-17.3	1.38			
3p	-9.2	1.38			
Pt 6s	-8.98	2.55			
6p	-4.18	2.53			
5d	-10.57	6.01	2.696	0.6333	0.5512
La 6s	-7.67	2.14			
6p	-5.01	2.08			
5d	-8.21	3.78	1.381	0.7765	0.4586

^a Exponents and coefficients in a double- ζ expansion of the 5d orbital.

$\text{Ca}^{2+}(\text{CuGe})^{2-}$. Neglecting the cation and filled d core, one may consider it equivalent to $(\text{GeGe}')^+$. There would be a hole in the π band, which would provide a driving force to form bonds between layers. The observed structure is shown in 25.

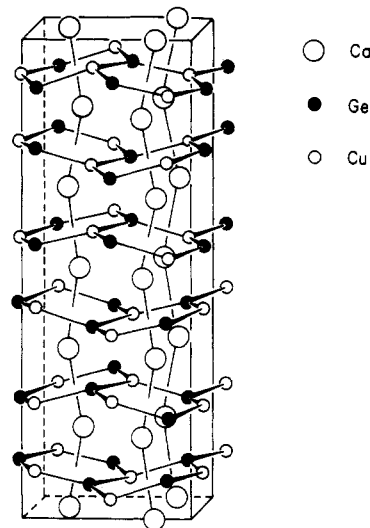
Finally, we show the DOS to LaPtSi calculated by including the cation La in Figure 8. Since La is more than 3.2 Å away from both Pt and Si, there is not much interaction between them. Figure 8 is essentially the DOS of PtSi net plus that of La. The DOS of PtSi is not changed much (cf. Figure 6). But around the Fermi level, there is a lot of contribution from La states. Thus, the presence of the cation will strongly affect the conducting and magnetic properties of the compound.

Acknowledgment. We thank Dr. Thomas Albright for a discussion, Joyce Barrows for the typing, and Jane Jorgensen for the drawings. Our research was generously supported by the National Science Foundation through Grant DMR8217227AO2 to the Materials Science Center at Cornell University.

Appendix

The extended Hückel method³² was used in the calculations.

- (26) Suzuoka, T.; Adelson, E.; Austin, A. E. *Acta Crystallogr. A* **1968**, *24*, 513.
 (27) Jeitschko, W. *Acta Crystallogr. B* **1975**, *31*, 1187.
 (28) Castelliz, L. *Monatsh. Chem.* **1953**, *84*, 765.
 (29) Eisenmann, B.; Cordier, G.; Schäfer, H. *Z. Naturforsch., B* **1974**, *29*, 457.
 (30) Evers, J.; Oehlinger, G. *J. Solid State Chem.* **1986**, *62*, 133.
 (31) Marazza, R.; Rossi, D.; Ferro, R. *J. Less-Common Met.* **1980**, *75*, P25.



CaCuGe

25

Since the extended Hückel total energy may not be reliable in situations where the distance is varied, we kept the Si-Si distance fixed at 2.414 Å (the distance in SrSi₂) and Si-Pt at 2.44 Å (ideal bond length in LaPtSi). Pt parameters were derived from charge iteration of LaPtSi, with 6 k points. 494 k points were used for the graphite and CaSi₂ structures, 396 for ThSi₂, 84 for SrSi₂, 494 for transition metal AlB₂ structure, 270 for LaPtSi, and 35 for LaIrSi. These are mesh points in the irreducible wedge of the Brillouin zone and were generated according to Pack and Monkhorst's method.³³ The extended Hückel parameters are listed in Table II.

Registry No. AlB₂, 12041-50-8; ThSi₂, 12067-54-8; LaPtSi, 81775-28-2.

- (32) (a) Hoffmann, R. *J. Chem. Phys.* **1963**, *39*, 1397. Hoffmann, R.; Lipscomb, W. N. *J. Chem. Phys.* **1962**, *36*, 2179; **1962**, *37*, 2872. Ammeter, J. H.; Bürgi, H.-B.; Thibeault, J. C.; Hoffmann, R. *J. Am. Chem. Soc.* **1978**, *100*, 3686. (b) Whangbo, M.-H.; Hoffmann, R.; Woodward, R. B. *Proc. R. Soc. London* **1979**, *A366*, 23.
 (33) Pack, J. D.; Monkhorst, H. *Phys. Rev. B* **1977**, *16*, 1748.

Contribution from the Departments of Chemistry, Baker Laboratory, Cornell University, Ithaca, New York 14853, and Rensselaer Polytechnic Institute, Troy, New York 12181

Electrocatalytic Activity of Electropolymerized Films of Bis(vinylterpyridine)cobalt(2+) for the Reduction of Carbon Dioxide and Oxygen

H. C. Hurrell,[†] A.-L. Mogstad,[†] D. A. Usifer,[‡] K. T. Potts,[‡] and H. D. Abruña^{*†}

Received July 29, 1988

Electropolymerized films of $[\text{Co}(\nu\text{-tpy})_2]^{2+}$ ($\nu\text{-tpy}$ = 4'-vinyl-2,2':6',2''-terpyridine) are active catalytically in the electroreduction of both carbon dioxide and oxygen. The polymer films lower the overpotential of carbon dioxide reduction in DMF by nearly 1.0 V and the four-electron reduction of oxygen in aqueous solution by 300 mV. The predominant product of carbon dioxide reduction is formic acid, as determined by the chromatographic acid test. The product distribution (water vs peroxide) in the reduction of oxygen was strongly dependent on the polymer coverage, with water being the predominant product at high coverage ($>2.5 \times 10^{-9}$ mol/cm²), whereas at lower coverage, hydrogen peroxide was the main reaction product.

Introduction

The reduction of carbon dioxide to useful fuel products and the four-electron reduction of oxygen to water at potentials close to those dictated by thermodynamics have attracted considerable interest in recent years.¹ These are particularly difficult reactions to catalyze because they involve multiple electron transfers that

are often coupled with other chemical steps, e.g. protonation, and in addition there can be other reaction pathways such as the

- (1) (a) Fisher, B.; Eisenberg, R. *J. Am. Chem. Soc.* **1980**, *102*, 7361. (b) Lieber, C. M.; Lewis, N. S. *J. Am. Chem. Soc.* **1984**, *106*, 5033. (c) Webley, W. S.; Durand, R. R.; Anson, F. C. *J. Electroanal. Chem. Interfacial Electrochem.* **1987**, *229*, 273. (d) Holdcroft, S.; Funt, B. L. *J. Electroanal. Chem. Interfacial Electrochem.* **1987**, *225*, 177. (e) Collin, J.-P.; Jouaiti, A.; Sauvage, J.-P. *Inorg. Chem.* **1988**, *27*, 1986. (f) Cabrera, C. R.; Abruña, J. *J. Electroanal. Chem. Interfacial Electrochem.* **1986**, *209*, 101.

[†] Cornell University.

[‡] Rensselaer Polytechnic Institute.

reduction of oxygen to hydrogen peroxide rather than water.

Catalysts immobilized on an electrode surface are particularly advantageous due to their ready separation from the reaction medium and the small amount of material necessary for reaction. In addition the reaction rate can be controlled by the applied potential. In the case of $[\text{Co}(\text{v-tpy})_2]^{2+}$ (v-tpy = 4'-vinyl-2,2':6',2''-terpyridine), the immobilization of the complex via electropolymerization to a polymer network on the surface also facilitates the electrochemical generation of an open coordination site on cobalt, which is generally regarded as a prerequisite for activation of small molecules such as oxygen and carbon dioxide. It appears that, for the polymeric film, steric constraints cause one (or both) of the terpyridine ligands to become bidentate. Such an open coordination site is then available for solvent or other small molecules such as oxygen or carbon dioxide to bind.² This is in marked contrast to the behavior of $[\text{Co}(\text{terpy})_2]^{2+}$ in solution, where the ligands always retain their tris coordination.

Numerous studies have been carried out on transition-metal complexes as reductive catalysts. In solution, $[\text{Ni}(\text{bpy})_3]^{2+}$, after being reduced to Ni^0 has been observed to reduce carbon dioxide to carbon monoxide.³ $[\text{Co}(\text{bpy})_3]^{2+}$ has been observed to reduce allyl halides electrocatalytically.⁴ Cobalt phthalocyanines adsorbed on carbon electrode surfaces have been shown to reduce carbon dioxide to carbon monoxide at potentials as low as -0.65 V vs SCE at pH 5.0, possibly through a mechanism involving a cobalt hydride intermediate.⁵

There have been numerous studies on the use of electrodes modified with Co porphyrins or phthalocyanines for the electrocatalytic reduction of oxygen. Recently, Murray et al. found that the catalytic activity of electrodes modified with films of cobalt tetrakis(*o*-aminophenyl)porphyrin complexes toward oxygen reduction was dependent on coverage, with higher coverages facilitating the four-electron reduction of oxygen.⁶ This was attributed to the formation of dimeric species at high coverage.

We have utilized electropolymerized films of $[\text{Co}(\text{v-tpy})_2]^{2+}$ in the electrocatalytic reduction of oxygen and carbon dioxide. The utility of surface-immobilized catalysts is dramatically evident, since the monomer in solution is catalytically inactive for these reductions at potentials where the immobilized layer is quite active.²

Experimental Section

Reagents. $[\text{Co}(\text{v-tpy})_2]^{2+}$ was prepared as described previously.⁷ Acetonitrile and dimethylformamide (DMF) (Burdick and Jackson distilled in glass) were dried over 4-Å molecular sieves. Tetra-*n*-butylammonium perchlorate (TBAP) (G. F. Smith) was recrystallized three times from ethyl acetate and dried under vacuum at 90 °C for 72 h. Water was purified by passage through a Milli-Q purification train. All other reagents were of at least reagent grade quality and were used without further purification.

Instrumentation. Electrochemical experiments were performed with either an IBM-EC225 potentiostat or a Pine Instruments Model RDE4 bipotentiostat, and coulometric measurements were made on a BAS 100 electrochemical analyzer. Data were recorded on a Soltec X-Y-Y recorder. Rotated disk and ring-disk electrode experiments were carried out on a Pine Instruments Model MSR rotating disk electrode assembly. Spectral measurements utilized a Hewlett Packard Model 8451 spectrophotometer.

Glassy-carbon rotated disk and glassy-carbon disk/platinum ring electrodes were shrouded with Teflon (Pine Instruments). The ring collection efficiency was 0.23 calibrated with measurements in a solution of ferrocene. Electrodes were polished prior to use with 1- μm diamond

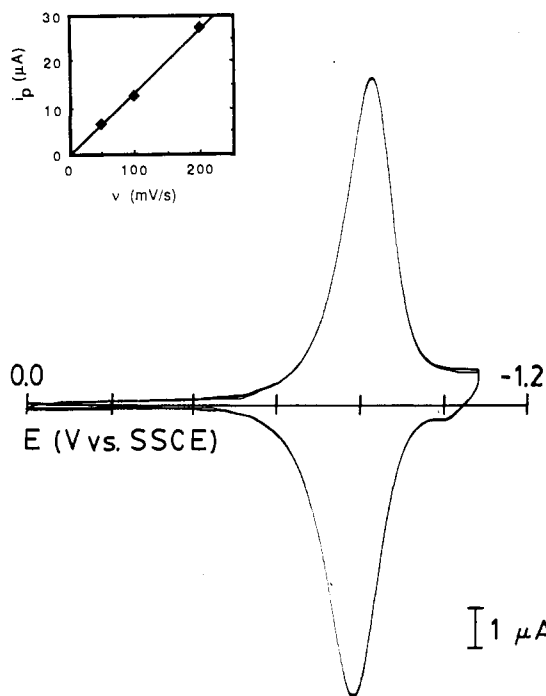


Figure 1. Cyclic voltammogram in acetonitrile/0.1 M TBAP at 50 mV/s for a glassy-carbon electrode modified with an electropolymerized film of $[\text{Co}(\text{v-tpy})_2]^{2+}$. Inset: plot of peak current vs sweep rate.

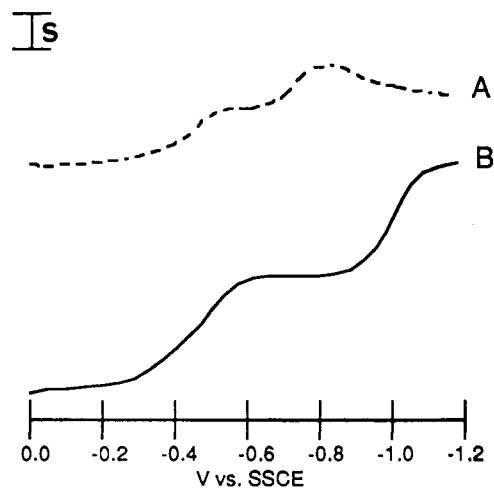


Figure 2. Linear-sweep voltammograms at 10 mV/s in oxygen-saturated aqueous pH 8.7 buffer solution ($\text{NaOH}/\text{Na}_2\text{HPO}_4$) for the reduction of dioxygen at an electrode modified with $[\text{Co}(\text{v-tpy})_2]^{2+}$ (A, $s = 50 \mu\text{A}$) and at a glassy-carbon electrode (B, $s = 10 \mu\text{A}$).

paste (Buehler) and rinsed thoroughly with water and acetone. Electrochemical cells were of conventional design. All potentials are referenced to the sodium saturated calomel electrode (SSCE) without regard for the liquid junction potential.

Procedures. Electrodes were modified with electropolymerized films of $[\text{Co}(\text{v-tpy})_2]^{2+}$ by scanning the potential (200 mV/s) between 0.0 and -1.70 V for a prescribed length of time (depending on the desired coverage) in a thoroughly degassed 1.0 mM solution of $[\text{Co}(\text{v-tpy})_2]^{2+}$ in acetonitrile with 0.1 M TBAP. The coverage of the polymer film was determined from the integrated charge of the cyclic voltammogram wave at a formal potential of -0.81 V when cycled in clean acetonitrile/0.1 M TBAP solution containing no dissolved complex.

Gases (presaturated with solvent) were vigorously bubbled through solutions for 45 min prior to experiments to ensure saturation. The concentration of oxygen in $\text{NaOH}/\text{Na}_2\text{HPO}_4$ aqueous buffer at pH 8.7 saturated with oxygen was 1.4 mM and in the ambient atmosphere was 0.3 mM at 1 atm and at 22 °C.⁸ The concentration of carbon dioxide in saturated DMF was 215 mM at 1 atm and at 22 °C.⁹

- (2) Guadalupe, A. R.; Usifer, D. A.; Potts, K. T.; Hurrell, H. C.; Mogstad, A.; Abruña, H. D. *J. Am. Chem. Soc.* **1988**, *110*, 3462.
- (3) Daniele, S.; Ugo, P.; Bontempelli, G.; Fiorani, M. *J. Electroanal. Chem. Interfacial Electrochem.* **1987**, *219*, 259.
- (4) Kamau, G. N.; Rusling, J. F. *J. Electroanal. Chem. Interfacial Electrochem.* **1988**, *240*, 217.
- (5) (a) Lieber, C. M.; Lewis, N. S. *J. Am. Chem. Soc.* **1984**, *106*, 5033. (b) Christensen, P. A.; Hamnett, A.; Muir, A. V. G. *J. Electroanal. Chem. Interfacial Electrochem.* **1988**, *241*, 361.
- (6) Bettelheim, A.; White, B. A.; Murray, R. W. *J. Electroanal. Chem. Interfacial Electrochem.* **1987**, *217*, 271.
- (7) Potts, K. T.; Usifer, D. A.; Guadalupe, A. R.; Abruña, H. D. *J. Am. Chem. Soc.* **1987**, *109*, 3961.

- (8) Linke, W. F. *Solubilities of Inorganic and Metallorganic Compounds*, 4th ed.; American Chemical Society: Washington, DC, 1965; Vol. 11, p 1229.

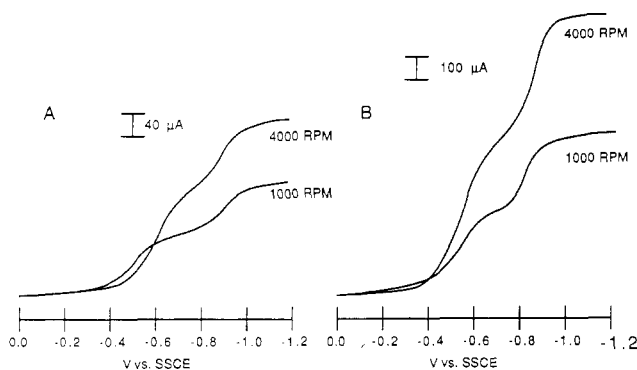


Figure 3. Rotating-disk voltammograms at 10 mV/s for the reduction of dioxygen in aqueous NaOH/Na₂HPO₄ pH 8.7 buffer solution at 1000 and 4000 rpm: (A) [O₂] = 0.3 mM; (B) [O₂] = 1.4 mM.

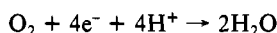
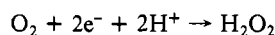
Electrolysis at -1.20 V in CO₂-saturated DMF solutions was carried out with a continuous flow of DMF-saturated carbon dioxide. The production of formic acid was estimated by using the chromotropic acid spot test¹⁰ and measuring the absorbances at 482 and 584 nm due to the reaction of chromotropic acid with formic acid. Absorbances were referenced to a bare electrode under the same conditions as a blank.

Results and Discussion

The electrochemistry of [Co(v-tpy)]²⁺ has been described previously.² Figure 1 shows a cyclic voltammogram (from 0.0 to -1.0 V) in acetonitrile/0.1 M TBAP under nitrogen for a glassy-carbon electrode modified with an electropolymerized film of [Co(v-tpy)]²⁺. The wave with an E° value of -0.81 V corresponds to the Co(II/I) couple. The wave shape is characteristic of a surface-confined reversible redox couple with the expected linear relationship of peak current with potential sweep rate (Figure 1 inset).

Oxygen Reduction Catalysis. Figure 2 shows voltammograms for a bare and [Co(v-tpy)]²⁺-modified glassy-carbon electrode in an oxygen-saturated aqueous NaOH/Na₂HPO₄ buffer solution at pH 8.7. Oxygen reduction occurs at E_p values of -0.60 and -1.10 V at the bare carbon electrode surface. At the modified electrode, however, these voltammetric waves are shifted to E_p values of -0.48 and -0.81 V, suggestive of electrocatalytic behavior. In media of lower pH, the second reduction wave was not observed. Other cobalt reduction catalysts have been found more effective in the four-electron reduction of oxygen to water in basic solutions than in acidic media.⁶

The electrocatalytic reduction was studied by rotated-disk voltammetry. Figure 3 illustrates the voltammetry at rotation rates of 1000 and 4000 rpm for a modified glassy-carbon electrode in atmospheric oxygen (A) and saturated oxygen solutions (B). The current is proportional to the concentration of oxygen in solution and is thus enhanced approximately 4-fold for the electrode in saturated oxygen solution, consistent with the difference in oxygen concentration. The waves at -0.50 and -0.80 V are ascribed to the reduction of oxygen to peroxide and to water, respectively.



The coverage of the polymer film greatly influenced which reduction peak dominated. For coverages up to $\Gamma = 2.5 \times 10^{-9}$ mol/cm² (approximately 25 equivalent monolayers), the two-electron reduction to peroxide dominated. Whereas for coverages beyond $\Gamma = 2.5 \times 10^{-9}$ mol/cm², the four-electron reduction to water becomes important, although both reduction processes still occur.

The assignment of the reduction processes is supported by rotated ring-disk electrode experiments. While reduction occurred

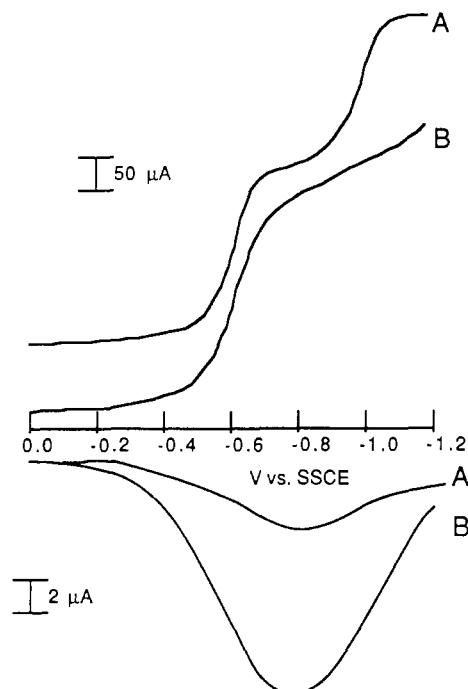


Figure 4. Disk and ring currents ($E_R = +1.35$ V vs SSCE) vs disk potential scanned at 10 mV/s for a glassy-carbon disk, platinum ring electrode rotated at 2500 rpm for the reduction of dioxygen in oxygen-saturated aqueous pH 8.7 buffer solution at a polymer-modified electrode at coverages of (A) 9.7×10^{-9} mol/cm² and (B) 2.4×10^{-9} mol/cm².

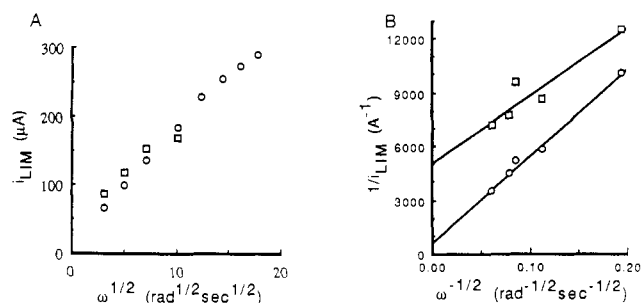


Figure 5. (A) Levich and (B) Koutecky-Levich plots for rotated-disk limiting currents at an electrode modified with [Co(v-tpy)]²⁺ at a coverage of 9.7×10^{-9} mol/cm² for the two-electron (○) and four-electron (□) reduction of dioxygen in aqueous pH 8.7 buffer solution.

at the disk, the ring potential was maintained at $+1.35$ V to oxidize, and thus monitor, any H₂O₂ produced at the disk. As the polymer film coverage was increased, the ratio of the ring current to the disk current decreased, indicating a diminution in the formation of hydrogen peroxide (Figure 4). At low coverage (3.4×10^{-10} mol/cm²), the H₂O₂ yield was 29.5% of the total reduction current, while at higher coverage (9.8×10^{-9} mol/cm²), the H₂O₂ yield decreased to 6.5% at 2500 rpm.

The transition from the two-electron reduction process (yielding peroxide) to two competing reduction pathways at higher coverages (yielding peroxide and water, respectively) may be related to the closer proximity of the Co centers at higher coverages. We have previously studied the concentration dependence of the metal complexes on coverage, and it exhibits an initial increase in concentration with varying coverage.² At high enough coverage, the concentration levels off. These findings indicate a change in packing density up to coverages of 15–20 monolayer equivalents, fully consistent with our observations. The four-electron reduction of oxygen to water may dominate when two Co centers can simultaneously contribute electrons. As mentioned previously, Murray et al.⁶ have recently reported on the reduction of oxygen at electrodes modified with films of cobalt tetrakis(*o*-aminophenyl)porphyrin in which the second reduction wave (the four-electron reduction to water) was enhanced while the two-electron reduction to peroxide diminished at higher coverages.

(9) Stephen, H.; Stephen, T. *Solubilities of Inorganic and Organic Compounds*; Pergamon Press: New York, 1963; Vol. 1, p 1063.

(10) Feigl, F. *Spot Test in Organic Analysis*; Elsevier: Amsterdam, 1956; p 451.

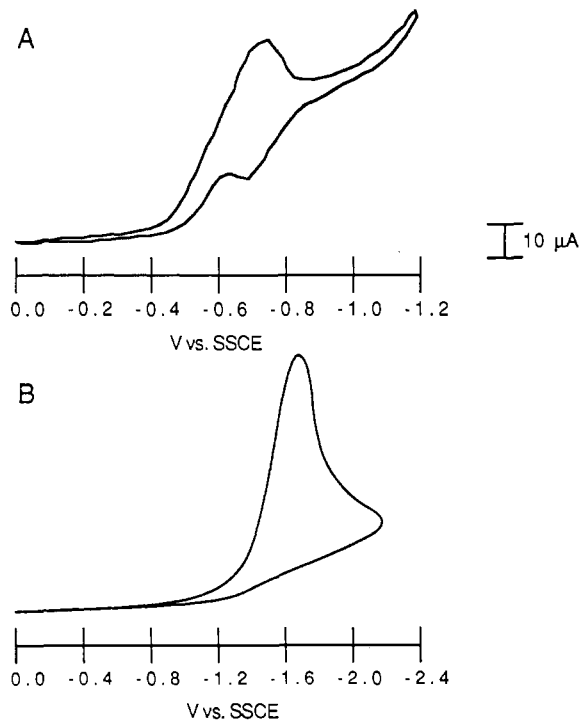


Figure 6. Rotated-disk voltammograms at 1000 rpm in CO_2 -saturated DMF/0.1 M TBAP solution for the reduction of carbon dioxide at (A) a $[\text{Co}(\text{v-tpy})_2]^{2+}$ -modified electrode and (B) a bare glassy-carbon electrode.

They attributed this enhancement to the formation of cobalt dimer species.

Limiting currents for each of the reduction processes are plotted as a function of $\omega^{1/2}$ in Figure 5A. The linearity of these plots at slower rotation rates indicates mass transport limited kinetics. At higher rotation rates, limiting currents level off, indicating some kinetic limitation such as a preceding chemical step, boundary layer effects, or limiting reactant permeation rates.

Assuming that electron transport through the polymer film is the limiting step for this reduction, the Koutecky–Levich equation can be applied:¹¹

$$1/i_{\text{lim}} = 1/(nFAk\Gamma C_b) + 1/(0.62nFA\nu^{-1/6}D^{2/3}\omega^{1/2}C_b)$$

where C_b is the bulk concentration of the reactant (oxygen) in water, Γ is the total surface coverage, ν is the kinematic viscosity, and ω is the rotation rate. In the determination of the rate constant, it was assumed that all of the deposited material was active in the reaction. This assumption, however, may not be valid at high coverages when reactant permeation may be limiting. Plots of $1/i_{\text{lim}}$ versus $\omega^{-1/2}$ are consistently linear (Figure 5B); $r = 0.98$. At coverages of $(5\text{--}10) \times 10^{-9}$ mol/cm², the second-order rate constants were $4 (\pm 1) \times 10^6 \text{ M}^{-1} \text{ s}^{-1}$ for the two-electron reduction and $3.6 (\pm 1) \times 10^5 \text{ M}^{-1} \text{ s}^{-1}$ for the four-electron reduction. These rate constants are averages of five replicate determinations and two concentrations of oxygen (1.4 and 0.3 mM). The diffusion coefficient of oxygen was determined from the slopes of the Koutecky–Levich plots to be $2.0 (\pm 0.8) \times 10^{-6} \text{ cm}^2/\text{s}$, which is significantly lower than its solution value and may indicate impeded permeation.

However, results from the reduction of carbon dioxide (vide infra) show linear Levich plots up to surface coverages of 1×10^{-8} mol/cm², so that the limiting factor in the reduction of oxygen may be the formation of a precursor rather than the rate of substrate permeation.

Carbon Dioxide Reduction Catalysis. The reduction of carbon dioxide was dependent on the nature of the solvent. Acetonitrile

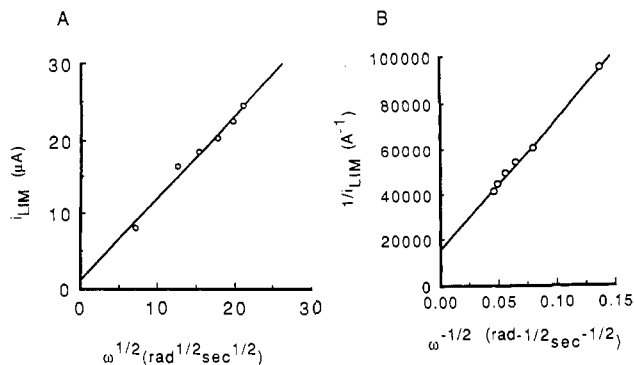


Figure 7. (A) Levich and (B) Koutecky–Levich plots for rotated-disk limiting currents at an electrode modified with $[\text{Co}(\text{v-tpy})_2]^{2+}$ at a coverage of 9.9×10^{-9} mol/cm² for the two-electron reduction of carbon dioxide in DMF/0.1 M TBAP.

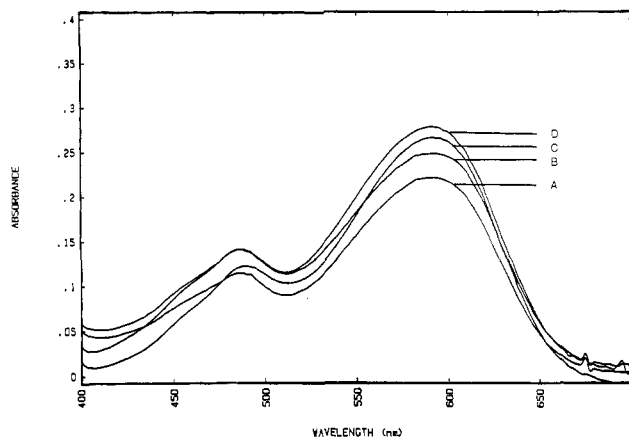


Figure 8. Absorption spectra for the reaction of formate with chromotropic acid after electrolysing a CO_2 -saturated DMF/0.1 M TBAP solution with a $[\text{Co}(\text{v-tpy})_2]^{2+}$ -modified platinum-gauze electrode after (A) 0.44, (b) 0.51, (C) 0.64, and (D) 1.10 C of charge.

coordinates effectively due to the π -acidity of the nitrile moiety. In such solvents, no catalysis of carbon dioxide reduction was observed, probably due to occupation of the cobalt coordination site by solvent. However, in less coordinating solvents such as DMF, a strong catalytic effect was present.

At electrodes modified with films of electropolymerized $[\text{Co}(\text{v-tpy})_2]^{2+}$ in solutions of DMF/0.1 M TBAP saturated with carbon dioxide, the reduction of carbon dioxide can be effected at -0.90 V (Figure 6A), which is nearly 1.0 V less negative than the corresponding value at a bare carbon electrode surface (Figure 6B).

Electrodes coated with about 1×10^{-8} mol/cm² were employed in these studies. At high coverage values, the permeation of carbon dioxide appeared to be impeded, thus reducing the relative catalytic activity of the films and resulting in deviations from linearity in the i_{lim} versus $\omega^{1/2}$ plots. Such plots were linear at high rotation rates for lower polymer film coverages (Figure 7A).

In order to analyze for products of the carbon dioxide reduction, the DMF/0.1 M TBAP solution was saturated with carbon dioxide and a continuous flow of DMF-saturated carbon dioxide was maintained through the system. The solution was electrolyzed at -1.20 V with a polymer-modified platinum gauze electrode for 4 h. Formic acid was detected as a reduction product by using the chromotropic acid spot test.⁹ Further experiments were carried out to determine the yield of formic acid by using UV/vis spectroscopy. The products of the chromotropic acid spot test have absorbances at 482 and 584 nm, and these were monitored to determine the quantity of formic acid produced as the reaction progressed (Figure 8).

Based on the production of formic acid, the turnover number for the catalyst was in excess of 500 turnovers. Chronocoulometry was carried out to assess the current efficiency of the system. The amount of the charge passed during electrolysis was compared

(11) (a) Levich, V. G. *Physicochemical Hydrodynamics*; Prentice-Hall: Englewood Cliffs, NJ, 1962; pp 345–357. (b) Koutecky, J.; Levich, V. G. *Zh. Fiz. Khim.* 1956, 32, 1565.

to the amount of charge consumed in the production of formic acid. The current efficiency of electropolymerized films was nearly 100%.

Both the turnover number and current efficiencies might be larger if other reduction products were also being formed during electrolysis. We have not yet detected products other than formic acid although initial studies by mass spectrometry detected traces of carbon monoxide. Also, the coverage of the platinum gauze is not known to a high degree of accuracy, and high coverages would preclude activity throughout the film.

After 1.1 C of charge was passed through the system, the electrochemistry of the catalyst was still present. However, the amount of electrochemically active material had been reduced to 25% of its initial value. The kinetics of the electrocatalytic carbon dioxide reduction were determined by using the Koutecky-Levich equation (analogous to the oxygen reduction kinetic analysis). The second-order rate constant for the reduction of carbon dioxide by two electrons is $1 (\pm 1) \times 10^3 \text{ M}^{-1} \text{ s}^{-1}$, as determined from the intercept of $1/i_{\text{lim}}$ versus $\omega^{-1/2}$ plots (Figure

7B). Although the rate constant for this reaction is not large, the decrease in the reduction potential due to the polymer film is remarkable.

The polymerized films of $[\text{Co}(\text{v-tpy})_2]^{2+}$ are capable of reducing carbon dioxide to formic acid and thus creating a carbon-hydrogen bond. We propose that carbon dioxide binds to the open coordination site at cobalt and is subsequently reduced. The generation of an open coordination site at cobalt is wholly responsible for this catalytic activity. If this assertion is correct, one would expect that a single quinquepyridine ligand bound to a cobalt center may be even more active. We are currently pursuing the study of the electrochemistry and electrocatalytic activity of $[\text{Co}(\text{v-qpy})]^{2+}$.

Acknowledgment. This work was generously funded by the National Science Foundation and the Materials Science Center at Cornell University. H.C.H. acknowledges support by a fellowship from the Aerospace Corp. H.D.A. is a recipient of a Presidential Young Investigator Award (1984-1989) and a Sloan Fellowship (1987-1989).

Contribution from the Department of Chemistry,
University of Queensland, Brisbane, Australia 4067

Synthesis and Characterization of (Catecholato)bis(β -diketonato)vanadium(IV) Complexes

Clifford J. Hawkins* and Themistoklis A. Kabanos¹

Received August 30, 1988

The syntheses of the complexes $[\text{V}(\text{cat})(\text{acac})_2]$, $[\text{V}(\text{cat})(\text{bzac})_2]$, and $[\text{V}(\text{dtbc})(\text{bzac})_2]$ are described, and the complexes' UV-visible, infrared, and mass spectral data are presented. The complexes are nonelectrolytes with a room-temperature magnetic moment of about $1.8 \mu_{\text{B}}$, consistent with the d^1 vanadium(IV) system. The complexes show reversible one-electron reduction to the vanadium(III) state at -0.22 , -0.26 , and -0.37 V (NHE), respectively, in acetonitrile and at -0.39 , -0.38 , and -0.56 V (NHE), respectively, in dichloromethane. Oxidation to the vanadium(V) state does not occur at potentials less positive than 1.0 V, at which the catecholate ligands undergo oxidation. These mixed-ligand vanadium(IV) complexes are more stable to disproportionation than the tris(catecholato) and tris(β -diketonato) complexes, more stable to oxidation than the former complexes, and more stable to reduction than the latter.

Introduction

Only a few non-vanadyl vanadium(IV) fully chelated species are well characterized.¹⁻⁶ This is surprising because these types of complexes provide access to a range of vanadium chemistries as they have, in principle, the possibility of oxidation and reduction to equivalent vanadium(V), -(III), and -(II) species, whereas the oxovanadium species are unable to retain their integrity after redox reactions. The only mixed-chelate complexes reported are $[\text{V}(\text{bpy})(\text{dtbc})_2]$ and $[\text{V}(\text{phen})(\text{dtbc})_2]$.^{7,8} This paper reports the

synthesis and characterization of mixed catecholate β -diketonate complexes and a comparison of the complexes' properties with those of the tris complexes of these ligands.

Experimental Section

Materials. Catechol and tetrabutylammonium perchlorate were recrystallized twice from ethanol, and 3,5-di-*tert*-butylcatechol was recrystallized from pentane. Sodium methoxide,⁹ oxobis(2,4-pentanedionato)vanadium(IV),¹⁰ oxobis(1-phenyl-1,3-butanedionato)vanadium(IV),¹¹ dichlorobis(2,4-pentanedionato)vanadium(IV),⁶ and dichlorobis(1-phenyl-1,3-butanedionato)vanadium(IV)⁶ were prepared by literature methods. All solvents were AnalaR grade. Methanol was dried by refluxing over magnesium methoxide, and hexane, toluene, pentane, dichloromethane, and acetonitrile were dried by refluxing over powdered calcium hydride. The distillation of the solvents was carried out under dried high-purity argon just prior to use. Vanadium analyses were carried out by atomic absorption spectroscopy, and the C, H, O analyses were conducted by the University of Queensland's microanalytical service.

For the syntheses of the complexes, all operations were carried out under dry, oxygen-free dinitrogen in a VAC Dri-Lab Model MO40-1 drybox unless otherwise stated.

- (1) On leave from the University of Ioannina, Ioannina, Greece.
- (2) Stiefel, E. I.; Dori, Z.; Gray, H. B. *J. Am. Chem. Soc.* **1967**, *89*, 3353.
- (3) Diamantis, A. A.; Snow, M. R.; Vanzo, J. A. *J. Chem. Soc., Chem. Commun.* **1976**, 264.
- (4) Cooper, S. P.; Koh, Y. B.; Raymond, K. N. *Inorg. Chem.* **1982**, *104*, 5092.
- (5) Comba, P.; Engelhardt, L. M.; Harrowfield, J. M.; Lawrance, G. A.; Martin, L. L.; Sargeson, A. M.; White, A. H. *J. Chem. Soc., Chem. Commun.* **1985**, 174.
- (6) Hambley, T. W.; Hawkins, C. J.; Kabanos, T. A. *Inorg. Chem.* **1987**, *26*, 3740.
- (7) Abbreviations: acac, 2,4-pentanedionate; bzac, 1-phenyl-1,3-butanedionate; cat, catecholate; dtbc, 3,5-di-*tert*-butyl-catecholate; bpy, 2,2'-bipyridine; phen, 1,10-phenanthroline; salen, bis(salicylaldiminato)-ethylenediamine; dike, β -diketonate.
- (8) Galeffi, B.; Postel, M. *Nouv. J. Chim.* **1984**, *8*, 481.

- (9) Baumgarten, H. E.; Petersen, J. M. *Organic Syntheses*; Wiley: New York, 1973; Collect. Vol. V, p 912.
- (10) Rowe, R. A.; Jones, M. M. *Inorg. Synth.* **1957**, *5*, 113.
- (11) Morgan, G. T.; Moss, H. W. *J. Chem. Soc.* **1913**, *103*, 78.